THE JOURNAL OF BIOLOGICAL CHEMISTRY
Vol. 277, No. 40, Issue of October 4, pp. 37023–37028, 2002
Printed in U.S.A.

Engineering of Metallothionein-3 Neuroinhibitory Activity into the Inactive Isoform Metallothionein-1*

Received for publication, June 10, 2002, and in revised form, July 11, 2002
Published, JBC Papers in Press, July 18, 2002, DOI 10.1074/jbc.M205730200

Núria Romero-Isart‡, Laran T. Jensen§, Oliver Zerbe¶, Dennis R. Winge§‖, and Milan Vašák‡‖

From the ‡Institute of Biochemistry, University of Zürich, Winterthurerstrasse 190, CH-8057 Zürich, Switzerland, the §Department of Biochemistry, University of Utah Health Science Center, Salt Lake City, Utah 84132, and the ¶Department of Pharmacy, ETH, Winterthurerstrasse 190, CH-8057 Zürich, Switzerland

The third isoform of mammalian metallothioneins (MT-3), mainly expressed in brain and down-regulated in Alzheimer's disease, exhibits neuroinhibitory activity *in vitro* and a highly flexible structure that distinguishes it from the widely expressed MT-1/-2 isoforms. Previously, we showed that two conserved prolyl residues of MT-3 are crucial for both the bioactivity and cluster dynamics of this isoform. We have now used genetic engineering to introduce these residues into mouse MT-1. The S6P,S8P MT-1 mutant is inactive in neuronal survival assays. However, the additional introduction of the unique Thr5 insert of MT-3 resulted in a bioactive MT-1 form. Temperature-dependent and saturation transfer ^{113}Cd NMR experiments performed on the ^{113}Cd-reconstituted wild-type and mutant Cd_7-MT-1 forms revealed that the gain of MT-3-like neuronal inhibitory activity is paralleled by an increase in conformational flexibility and intersite metal exchange in the N-terminal Cd_3-thiolate cluster. The observed correlation suggests that structure/cluster dynamics are critical for the biological activity of MT-3. We propose that the interplay between the specific Pro-induced conformational requirements and those of the metal-thiolate bonds gives rise to an alternate and highly fluctuating cluster ensemble kinetically trapped by the presence of the ^{5}TCPCP^{9} motif. The functional significance of such heterogeneous cluster ensemble is discussed.

Alzheimer's disease (AD)[1] is a complex cerebral disorder characterized by a progressive dysfunction, dystrophy, and death of neurons. The neuronal loss is accompanied by the formation of neurofibrillary tangles and senile (neuritic) plaques (1) and by a massive dendritic sprouting in AD brain (2). The underlying relationship between the various pathological factors has still to be fully resolved, but several potential contributors to the disease process have been identified. For instance, presenilins mediate the altered cleavage of the β-amyloid precursor protein to yield the amyloid peptide, which is the principal component of neuritic plaques (3). Other biomolecules have also been examined with regard to their association with AD. One potential factor is metallothionein-3 (MT-3), a member of the family of mammalian metallothioneins (4–6). This protein, also termed neuronal growth inhibitory factor, is expressed almost exclusively in the central nervous system and possesses neuroinhibitory properties *in vitro* that distinguish it from the MT-1 and MT-2 isoforms, also expressed in the central nervous system (7). Thus, MT-3, but not MT-1/-2, antagonizes the ability of AD brain extract to stimulate survival and neuritic sprouting of cultured neurons. Independently, MT-3 was also found to affect significantly the migration of cultured astrocytes (8). Neuronal inhibitory activity, which maps to the N-terminal domain (residues 1–30) of the protein (9, 10), has been established for Cu_4,Zn_3-MT-3 isolated from human (7) and bovine brains (11) and for recombinant human (9, 12, 13) and mouse Zn_7-MT-3 (9). In these studies, the effect of free zinc on the bioactivity could be excluded. In addition, changes in MT-3 mRNA levels in response to central nervous system injury have been taken to indicate an important role of the protein in brain repair (14, 15). In this context, it should be noted that MT-3-deficient mice showed no neuropathology under normal conditions but a higher susceptibility to seizures induced by kainic acid (16). The latter has been associated with the ability of MT-3 to prevent glutamate neurotoxicity *in vitro* (17).

MT-3 displays several other unique properties not found for MT-1/-2. Thus, it protects cultured cortical neurons from the toxic effect of amyloid β peptides (18) and is not induced by the typical inducers of MT-1/-2 biosynthesis such as metal ions (zinc, cadmium, and copper), hormones, inflammation-related stimuli, and stressful agents (19, 20). MT-3 was originally identified as an astrocytic component, but subsequent studies have demonstrated its expression in hippocampal glutaminergic neurons that release zinc from synaptic terminals (21). Moreover, constitutive expression of MT-3, but not MT-1, inhibits the growth of cultured kidney cells under zinc-deficient conditions (22). The characteristic physiological function of MT-3 is further supported by *in vivo* studies, in which mice overexpressing MT-3 in most organs died as a result of pancreatic atrophy, whereas expression of similar amounts of MT-1 had no effect (23). In AD, the absence or a significant decrease of MT-3 has been linked to the initiation of neuritic sprouting extension in an attempt to re-establish synaptic connections (7). In this instance, a potential cascade may cause the affected neurons to overextend themselves and eventually die. Since the discovery of MT-3 as a factor reduced in AD brains, there have been several conflicting reports (7, 8, 13, 24) with regard to AD-related changes of MT-3 levels. However, a recent comprehensive study (25) at both the protein and RNA level on a large sample size provides clear evidence of its down-regulation in AD brains.

Compared with the amino acid sequences of MT-1/-2 (61–62 amino acids), that of MT-3 (68 amino acids) shows ~70% se-

* This work was supported by Swiss National Science Foundation Grant 31-58858.99 (to M. V.), National Institutes of Health Grant ES03817 (to D. R. W), and Fundación Ramón Areces Spain postdoctoral fellowship (to N. R. I.). The costs of publication of this article were defrayed in part by the payment of page charges. This article must therefore be hereby marked "*advertisement*" in accordance with 18 U.S.C. Section 1734 solely to indicate this fact.

‖ To whom correspondence may be addressed.

[1] The abbreviations used are: AD, Alzheimer's disease; HSQC, heteronuclear single quantum correlation; MCD, magnetic circular dichroism; MT, metallothionein; UV, electronic absorption spectroscopy.

TABLE I
Comparison of the amino acid sequences of MT-3, MT-1, and the MT-1 site-directed mutants
The novel and conserved Thr 5, Pro 7, and Pro 9 of MT-3 are in boldface.

***β*-Domain**			
Mouse MT-1	1	MDPN·CSCSTGGSCTCTSSCACKNCKCTSCK	30
S6P,S8P MT-1	1	MDPN·C**P**C**P**TGGSCTCTSSCACKNCKCTSCK	30
S6P,S8P+T5 MT-1	1	MDPN**T**C**P**C**P**TGGSCTCTSSCACKNCKCTSCK	31
Human MT-3	1	MDPE**T**C**P**C**P**SGGSCTCADSCKCEGCKCTSCK	31
***α*-Domain**			
Mouse MT-1	31	KSCCSCCPVGCSKCAQGCVCKG·····AADKCTCCA	61
Human MT-3	32	KSCCSCCPAECEKCAKDCVCKGGEAAEAEAEKCSCCQ	68

quence identity and contains two inserts as follows: a Thr at position 5 and a Glu-rich hexapeptide in the C-terminal region (Table I). In addition, all known MT-3 sequences contain the conserved ^{6}CPCP^{9} motif, which is absent in all other members of the MT family (7, 19). Structural data have shown that, similar to MT-1/-2 (26, 27), M^{II}_7-MT-3 possesses two protein domains each encompassing a metal-thiolate cluster as follows: a 3-metal cluster, $M^{II}_3Cys_9$, located in the N-terminal β-domain (residues 1–30), and a 4-metal cluster, $M^{II}_4Cys_{11}$, in the C-terminal α-domain (residues 31–68) (28, 29). However, markedly increased structural flexibility and cluster dynamics were observed in the biologically active MT-3 compared with MT-1/-2 (28, 29). Consequently, whereas the solution structure of the α-domain of mouse Cd_7-MT-3 could be determined from NMR data, the dynamic disorder encountered in the β-domain prevented its direct structure determination (29). Most interestingly, mutation of the distinct ^{6}CPCP^{9} motif of MT-3 to ^{6}CSCA^{9} found in MT-2 was shown to abolish the inhibitory activity of the protein without altering its metal binding affinity but profoundly affecting the dynamics of the β-domain (9, 30). These findings have led to the proposal that the bioactivity of MT-3 stems from the distinct sequence motif and structure dynamics unique to this isoform (30).

To gain additional insight into the structural features responsible for the marked differences in biological activity between MT-1/-2 and MT-3, we have engineered the conserved ^{5}TCPCP^{9} sequence of MT-3 into the inactive and structurally well characterized Zn_7-MT-1 isoform, and we examined the biological and structural consequences. The neuronal bioassays with the S6P,S8P and S6P,S8P+T5 mutants of MT-1 revealed that the two conserved Pro residues together with the Thr insert are necessary and sufficient for biological activity. Moreover, as manifested by ^{113}Cd NMR studies on the ^{113}Cd-substituted MT-1 forms, the mutations introduced structural dynamics similar to that previously observed in the β-domain of $^{113}Cd_7$-MT-3. These findings provide evidence that both the presence of the ^{5}TCPCP^{9} motif and derived structure/cluster dynamics are essential for biological activity of MT-3.

EXPERIMENTAL PROCEDURES

Expression and Purification of MT-1 and Mutant Forms—Mouse MT-1 cDNA was amplified by PCR using a mouse liver cDNA library, generously provided by Dr. John Weis (University of Utah), as a template. Mutations in MT-1 at positions corresponding to residues Pro-7, Pro-9, and the Thr-5 insert in the MT-3 sequence were constructed by PCR mutagenesis, generating two MT-1 mutant forms: S6P,S8P MT-1 and S6P,S8P+T5 MT-1. The PCR products all contained 5′ *Nco*I and 3′ *Bam*HI sites and were subcloned into pET-3d (Novagen) for expression in *Escherichia coli* strain BL21(pLysS). The recombinant proteins were expressed as described previously (28) but extending the *E. coli* culture growth period to 12 h before harvesting the cells. Subsequent protein purification was as described for MT-3 (28) with the following changes. After gel filtration on Superdex 75, MT-1-containing fractions were loaded on a DEAE-MemSep-1500 cartridge (Millipore) equilibrated with 25 mM Tris/HCl and 50 mM NaCl at pH 8.0, and Zn_7-MT-1 was collected in flow-through fractions. The purity of the protein was verified by analytical C_{18} reversed phase-high pressure liquid chromatography and electrospray ionization mass spectrometry (Sciex API III$^+$) as described (28). The single T5A and ΔT5 (deletion) mutants of human MT-3, used in biological assays, were prepared as described (9).

Reconstituted Zn_7- and Cd_7-MT-1 forms were generated by the method of Vašák (31). Metal-to-protein ratios were determined by measuring the metal content by atomic absorption spectrometry (Instrumental Laboratories Video 12) and that of the protein via sulfhydryl quantification (20 Cys per protein) with 2,2′-dithiopyridine (32). In all cases, a metal-to-protein ratio of 7 ± 0.3 was obtained. To prepare samples suitable for NMR, the $^{113}Cd_7$-MT-1 protein solution in 25 mM Tris/HCl, 50 mM NaCl, pH 8.0, was concentrated by ultrafiltration (Amicon, YM1 membrane), freeze-dried, and redissolved in 0.5 ml of D_2O to yield an ~3 mM protein sample. Prior to and after NMR measurements the sample homogeneity was checked by analytical gel filtration on a Superdex 75 column (1 × 30 cm).

Spectroscopic Measurements—Electronic absorption (UV) spectra were recorded on a Varian Cary 3 spectrometer. CD and magnetic CD (MCD) measurements were carried out on a Jasco J-715 spectropolarimeter equipped with a 1.5 tesla electromagnet for room temperature MCD measurements. 133-MHz ^{113}Cd NMR spectra were recorded at both 298 and 323 K on a Bruker DMX-600 spectrometer using inverse-gated broad band proton decoupling, a 62,300-Hz spectral width, 0.13-s acquisition time, and 2-s pulse repetition rate (averaging 28,000 free induction decays per spectrum). The spectra were referenced against the temperature-corrected chemical shift of the external standard 0.1 M $Cd(ClO_4)_2$. The reversibility of the heat-induced changes in the spectra was confirmed by re-measuring the NMR spectra at 298 K after keeping the sample for 20 h at 323 K.

Cadmium-cadmium exchange was investigated by means of saturation transfer NMR experiments recorded at 315 K. This temperature was chosen because of better signal-to-noise ratio and reduced signal overlap compared with room temperature experiments. In these measurements, each ^{113}Cd ion of the $^{113}Cd_3S_9$ cluster in the β-domain was selectively saturated by a low power irradiation (field strength, $\gamma B_1/2\pi = 25$ Hz; duration, 100 ms). The resulting intensity reductions of the non-irradiated resonances in the ^{113}Cd NMR spectrum were monitored.

Neuron Survival Assay—Neonatal rat cortical cell cultures were prepared and maintained as described previously (9, 13). The cells were plated into serum-free minimum Eagle's N2 medium. Approximately 1 h later, the cultures were supplemented with one of the following: AD brain extract (240 μg of protein ml^{-1}), purified Zn_7-MT-1/-3 (< 20 μg/ml) dissolved in sterile phosphate-buffered saline solution, or both AD brain extract and MT. AD brain extract was freshly prepared as described previously (13) from the frontal cortex of human brain fulfilling all criteria for the diagnosis of AD. The number of surviving neurons was quantified after 3 days by microscopic examination of four random fields. Samples were tested in duplicate in three independent trials. All cell culture studies were carried out with the Zn(II)-containing forms as Cd(II) ions are neurotoxic.

RESULTS

Bioactivity of Mouse MT-1 and Its Mutant Forms—Although the original discovery of MT-3 neuronal growth inhibitory (7) could be verified in a number of laboratories (9, 11, 13), the origin of the bioactivity is still largely unknown. Nevertheless, the neuronal bioassay proved to be effective in reporting distinct properties of this isoform. Previous biological studies and mutational analysis on recombinant human Zn_7-MT-3 clearly established the necessity of both conserved proline residues (Pro-7 and Pro-9) for the neuronal growth inhibitory activity only exhibited by this MT isoform (9, 30). To shed light on the biological role of these residues, we have introduced them by site-directed mutagenesis into the biologically inactive MT-1

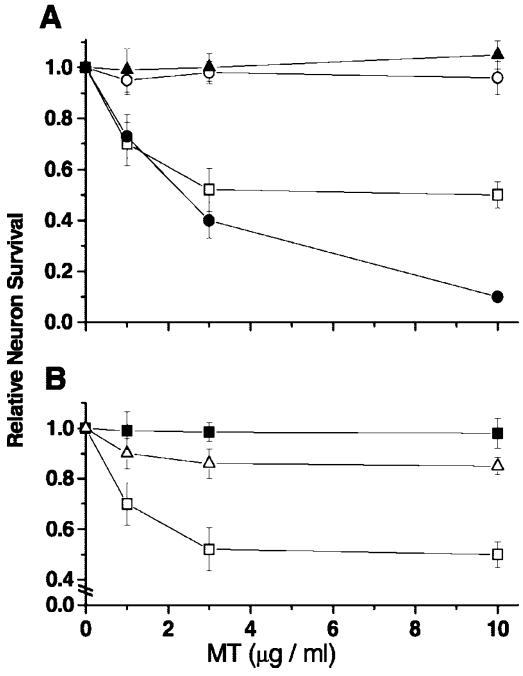

FIG. 1. **Generation of neuronal growth inhibitory activity in recombinant mouse Zn_7-MT-1 (*A*) and effect of Thr-5 in MT-3 bioactivity (*B*).** Wild-type MT-1 (○), S6P,S8P MT-1 (▲), S6P,S8P+T5 MT-1 (●), T5A MT-3 (△), and ΔT5 MT-3 (■) were tested for their ability to inhibit the survival of cortical neurons supplemented with AD brain extract. The active human Zn_7-MT-3 (□) is included for comparison. Relative survival (means ± S.E.) was determined by dividing the number of neurons per field in the presence of added MT by the number of neurons per field in the absence of added MT.

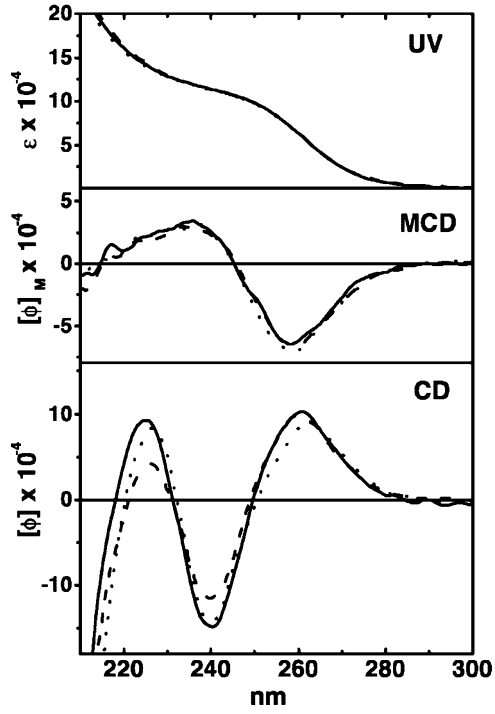

FIG. 2. **UV, CD, and MCD spectra of mouse Cd_7-MT-1 (···), Cd_7-S6P,S8P MT-1 (—), and Cd_7-S6P,S8P+T5 MT-1 (- - - -).** Conditions: 10 μM protein sample in 25 mM Tris/HCl, 50 mM NaCl, pH 8.0. UV, CD, and MCD spectra are expressed as ϵ (M^{-1} cm^{-1}), molar ellipticity $[\theta]$ (degree $dmol^{-1}$ cm^2) and $[\theta]_M$ (degree $dmol^{-1}$ cm^2 $tesla^{-1}$), respectively.

isoform, *i.e.* S6P,S8P MT-1 mutant. The relative survival of the cultured neurons as a function of increasing concentrations of added proteins is depicted in Fig. 1. As displayed, no biological activity was found with the S6P,S8P MT-1 mutant. In the next step, Thr-5 was inserted into S6P,S8P MT-1 giving rise to a mutant form, S6P,S8P+T5 MT-1, containing the conserved motif of MT-3, *i.e.* ^{5}TCPCP^9 (Table I). In the neuronal bioassay, this second mutant showed a biological activity similar to that seen with the MT-3 isoform (Fig. 1). Whereas at high protein concentrations the growth inhibition of MT-3 reached a plateau at about 50% of relative neuron survival, the inhibition by the bioactive MT-1 mutant steadily increases. The necessity of the Thr insert for biological activity of MT-1 is striking. Therefore, its effect on the activity of human MT-3 was also examined. Corresponding mutational and biological analysis showed that deletion of Thr-5 causes a loss, and its substitution to alanine greatly reduces bioactivity (Fig. 1). Taken together, these studies clearly demonstrate that both the two conserved Pro residues together with the Thr insert of the β-domain of MT-3 are necessary and sufficient for the neuronal growth inhibitory activity exhibited by this MT isoform.

Electronic Absorption, CD, and MCD Studies—To examine the structural changes associated with the gain of biological activity, the optical and magneto-optical properties of wild-type MT-1, S6P,S8P MT-1, and S6P,S8P+T5 MT-1, in their zinc- and cadmium-bound forms, were compared. Because of the increased covalence of the Cd–S bond, the characteristic CysS-Cd(II) ligand-to-metal charge transfer bands of cadmium-substituted MTs are substantially red-shifted from the region of the peptide backbone transitions (λ <230 nm) when compared with those in the zinc-containing MTs (33). In addition, the generation of ^{113}Cd derivatives allows the structure of the zinc centers to be probed by ^{113}Cd NMR (34). Therefore, only the spectra of cadmium-substituted MT-1 forms are shown (Fig. 2), although similar spectral changes have also been seen with the zinc-containing MT-1 derivatives. The validity of this approach is supported by the three-dimensional NMR structures of Zn_7-MT-2 and Cd_7-MT-2 from human liver, showing identical polypeptide fold (35). Moreover, the absence of ^{113}Cd chemical shift changes between resonances from the α-domain of wild-type MT-1 and its mutants (see below) indicates that structural changes in the MT-1 mutants are restricted to the 3-metal thiolate cluster of the β-domain.

The electronic absorption and MCD features of both mutated proteins are similar to those of wild-type Cd_7-MT-1. All show characteristic absorption spectra with shoulders at 250 nm (ϵ $\sim 1 \times 10^5$ M^{-1} cm^{-1}), due to CysS-Cd(II) ligand-to-metal charge transfer transitions (36), and a biphasic MCD profile, with extrema at −259 and +235 nm, ascribed to tetrahedrally coordinated $Cd(SCys)_4$ units (37). In contrast, the corresponding CD spectra, which unlike UV and MCD are highly sensitive to the cluster geometry and conformation of the enfolding polypeptide chain, reveal a small blue shift and slight intensity changes of the derivative CD profile of Cd_7-MT-1 upon S6P,S8P mutation (Fig. 2). Interestingly, in the previous CD studies of human Cd_7-MT-3, replacement of the two conserved prolines with the amino acids found in MT-2 (P7S,P9A) resulted in the opposite CD effects (30). After insertion of Thr-5 into S6P,S8P MT-1, no additional chiroptical changes have been discerned (Fig. 2). Consequently, the obtained data point to an alteration of the Cd_3S_9 cluster in the β-domain of MT-1 upon incorporation of the two proline residues found in MT-3. This conclusion is consistent with our previous zinc *K*-edge extended x-ray absorption fine structure studies on Zn_7-MT-3 and Zn_3-βMT-3 (38). In view of the CD changes between wild-type MT-1 and its mutants, the solvent accessibility/reactivity of their metal-ligating cysteines was assessed by monitoring changes in absorption related to the reaction with the electrophilic sulfhydryl reagent 5,5′-dithiobis-(2-nitrobenzoic acid) at 412 nm as a function of time (39). Yet no differences were found (data not

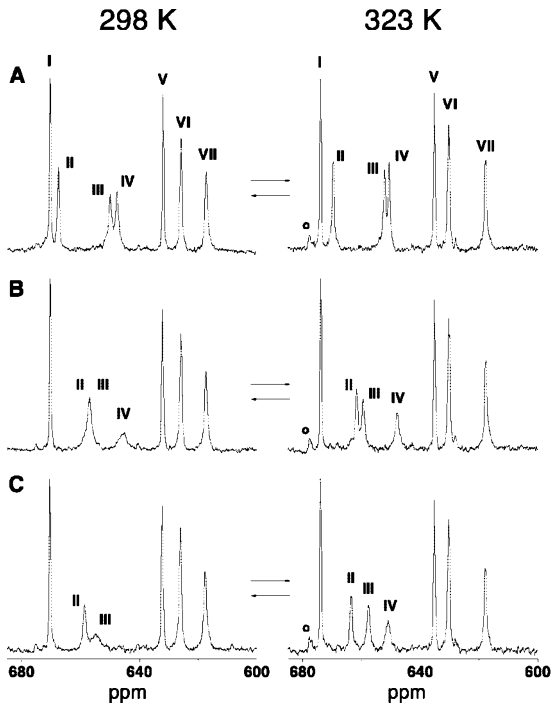

FIG. 3. **133-MHz ^{113}Cd NMR spectra of mouse $^{113}Cd_7$-MT-1 (*A*), $^{113}Cd_7$- S6P,S8P MT-1 (*B*), and $^{113}Cd_7$-S8P,S8P+T5 MT-1 (*C*) at 298 and 323 K.** 20-Hz line broadening was applied during processing. The *arrows* indicate the reversibility of the process. The small signals (○) are irreversible and originate from minor sample degradation during the measurement at 323 K.

shown). Similar results as to the solvent accessibility/reactivity of the metal-ligating cysteines in MT-3 and MT-1 have been found (9).

^{113}Cd NMR Studies—More detailed information regarding the structural influence of the mutations in the β-domain of MT-1 can be drawn from ^{113}Cd NMR studies. The slight structural differences among the seven binding sites in mammalian MTs create enough spectral dispersion to allow separate ^{113}Cd signals to be detected due to each metal-binding site. The ^{113}Cd NMR spectrum of wild-type mouse $^{113}Cd_7$-MT-1 is shown in Fig. 3*A*. The three-dimensional structure of this protein has recently been determined by NMR (27). Accordingly, the ^{113}Cd signals I and V–VII can be assigned to the Cd_4Cys_{11} cluster in the C-terminal α-domain of $^{113}Cd_7$-MT-1, and the remaining three minor signals (II–IV) to the Cd_3S_9 cluster in the N-terminal β-domain of the protein. The larger line width and lower intensity of the resonances originating from the 3-metal cluster compared with those of the 4-metal cluster reflect the enhanced flexibility of this domain (27). The first ^{113}Cd NMR check of the S6P,S8P MT-1 mutant at 298 K revealed a dramatic effect of the mutation on the intensity and line width of the ^{113}Cd resonances of the β-domain (Fig. 3*B*), indicating the existence of dynamic processes. As the Cd_4Cys_{11} cluster resonances remained unaffected by these mutations, further studies focused on the dynamics of the Cd_3S_9 cluster in the β-domain. In these studies, the effect of temperature and intersite metal exchange in the 3-metal cluster upon protein mutation were analyzed.

Comparative ^{113}Cd NMR analysis show that the S6P,S8P mutation leads to significant line broadening and signal intensity reduction of the MT-1 β-domain resonances at 298 K (Fig. 3*B* and Table II) and that both effects become more severe after additional insertion of Thr-5 (Fig. 3*C*). The latter, along with variations in chemical shift due to the sequence modification, results in overlap of signal III and signal II in S6P,S8P MT-1 and non-detection of signal IV in S6P,S8P+T5 MT-1. The corresponding spectra of wild-type and mutated proteins recorded at 323 K revealed marked changes in both the chemical shift and/or line width of the ^{113}Cd resonances (signals II–IV) of the β-domain, whereas those of the α-domain were virtually unaffected (Fig. 3 and Table II). Apart from the line sharpening due to decreased correlation time, which also affects signals from the α-domain, the resonances of the 3-metal cluster experience a temperature-dependent chemical exchange contribution to both their shifts and their line widths. This effect is substantially more pronounced in the spectrum of $^{113}Cd_7$-S6P,S8P MT-1 and even more in that of $^{113}Cd_7$-S6P,S8P+T5 MT-1. In both cases, this temperature-dependent modulation of the β-domain resonances allowed the three signals (II–IV) to be discerned at 323 K. In addition, a striking temperature effect on the intensity of the β-domain resonances in the mutants occurred compared with the wild-type protein. Thus, if calculating the total integrated area of the β resonances (II–IV) relative to that of the α domain (I and V–VII) and normalizing for the number of cadmium sites, in $^{113}Cd_7$-S6P,S8P MT-1 the area of the β signals at 323 K accounts for only 60% (47% at 298 K) of the total cadmium present. This value decreases to 45% (38% at 298 K) in the bioactive form $^{113}Cd_7$-S6P,S8P+T5 MT-1. Conversely, in the wild-type protein, 81% of the total expected β signal intensity is detected at 323 K (74% at 298 K). The observed behavior indicates that a substantial part of the signal intensity from the Cd_3S_9 cluster of the MT-1 mutants remains undetected under the conditions employed. It may be noted that no additional resonances were detected outside the chemical shift range presented and that the proteins were fully metal-loaded (see above). A similar behavior for ^{113}Cd NMR resonances of the Cd_3S_9 cluster in the β-domain has been observed in our previous studies on the bioactive human $^{113}Cd_7$-MT-3 (28). These features have been interpreted in terms of dynamic events involving *coupled* fast and slow exchange processes, on the ^{113}Cd chemical shift time scale, between conformational and/or configurational cluster substrates in the N-terminal β-domain of the protein (28, 30). Thus, minor sub-millisecond changes of the metal coordination geometry would be responsible for line broadening and would place these events in the fast exchange regime. The additional *coupled* slow exchange processes are connected to major structural alterations which, in turn, lead to the development of more extended configurational cluster fluctuations. The latter can be visualized as the temporary breaking and reforming of the metal-thiolate bonds (28, 40). Accordingly, the detected ^{113}Cd signals of the β-domain reflect only a part of the cluster population, whereas the ^{113}Cd signals of the majority of configurational cluster substrates remain undetected, because of an extensive exchange broadening and/or to their low population. Consequently, the incorporation of two Pro residues into the structure of MT-1 (S6P,S8P) introduces NMR features already observed for the bioactive MT-3 (28). Hence, it appears that the two-conserved Pro in MT-3 introduce a rate-limiting step in the exchange kinetics between the detectable and non-detectable ensemble of interchanging cluster substrates. This conclusion is supported by our previous studies on the biologically inactive double mutant P7S,P9A MT-3, in which a major part of the Cd_3S_9 cluster signal intensity could be recovered by raising the temperature (30). In addition, the present data reveal the contribution of Thr-5 to the dynamics of the MT-3 β-domain. Thus, the subsequent mutational insertion of Thr-5 into S6P,S8P MT-1 further contributes to line broadening and intensity reduction of ^{113}Cd resonances originating from the 3-metal cluster (Fig. 3*C*).

Despite the large thermodynamic stability of the metal-thiolate bonds in MTs, they are kinetically very labile. The occur-

TABLE II

^{113}Cd NMR chemical shift, δ (ppm), line width, Δν (Hz), and relative intensity, I (%) of ^{113}Cd signals in $^{113}Cd_7$-MT-1 (α- and β-domain) and the site-directed mutants at 298 and 323 K.

The integral of signal I was set to 100%. Spectra recorded with a 3 s repetition rate gave identical signal intensities, thereby ruling out signal saturation.

	MT-1						S6P,S8P MT-1						S6P,S8P+T5 MT-1					
	298 K			323 K			298 K			323 K			298 K			323 K		
	δ	Δν	I	δ	Δν	I	δ	Δν	I	δ	Δν	I	δ	Δν	I	δ	Δν	I
α																		
I	671	87	100	674	84	100	671	88	100	674	87	100	671	93	100	674	92	100
V	632	85	78	635	85	96	632	94	90	635	92	102	632	97	93	635	96	89
VI	626	129	86	630	112	105	626	131	98	631	125	120	626	126	111	630	125	105
VII	618	147	82	618	120	91	618	151	90	618	135	103	618	158	91	618	149	90
β																		
II	668	112	62	670	105	86	658	256[b]	96[b]	662	139	66	659	148	112[b]	664	133	44
III	650	168	67	652	115	74				660	167	61	655	510		658	133	45
IV	648	169	62	651	114	79	646	403	37	648	201	64	ND[c]	ND	ND	651	251	40

[a] Apparent line width of the unresolved signals.
[b] Total intensity of the unresolved signals.
[c] ND, not detected.

rence of intersite metal exchange in the 3-metal cluster of the β-domain in $^{113}Cd_7$-MT-1/MT-2 has been established by saturation transfer experiments (27, 41). In these experiments, irradiation of a single cadmium resonance will cause reduction in intensity of the non-irradiated resonances due to transfer of saturation to other metal sites, providing that metal exchange takes place during irradiation. The presence of such a metal exchange has been interpreted in terms of increased structure flexibility. Therefore, to explore further the dynamic events in the MT-1 structure generated by introducing the MT-3 motif, ^{5}TCPCP^{9}, ^{113}Cd exchange dynamics have been examined by saturation transfer experiments performed at 315 K. The results summarized in Table III indicate that the rate of intersite metal exchange in the Cd_3S_9 cluster of MT-1 follows the order S6P,S8P+T5 MT-1 > S6P,S8P MT-1 > wild-type MT-1. The substantially higher kinetic lability of the cadmium–thiolate bonds in the MT-1 mutants is also supported by the broadening and low intensity of the ^{113}Cd-^{1}H cross-peaks in the heteronuclear single quantum correlation ([^{113}Cd,^{1}H]-HSQC) spectra (data not shown). The latter effect hampered the comparative analysis of metal exchange by the HSQC-type saturation experiment (27) because of highly efficient transverse ^{113}Cd relaxation. Overall, the saturation transfer experiments provide additional evidence for the configurational entropy and noncompactness of the metal core in the β-domain of the generated MT-1 mutant forms. Taken together, the obtained NMR data are, on the one hand, in full agreement with the previously developed dynamic structural model for the β-domain in MT-3 (28, 30) and, on the other, allow delineation of the specific contribution of the two Pro and Thr residues to the significantly enhanced protein dynamics.

TABLE III

Saturation transfer between ^{113}Cd resonances in the β-domain of MT-1 and its site-directed mutants at 315 K

Cd saturated[a]	Cd observed	Residual intensity %		
		MT-1	S6P,S8P	S6P,S8P+T5
II	III	55	14	6
	IV	46	27	8
III	II	47	23	13
	IV	34	39	15
IV	II	45	36	23
	III	38	36	30

[a] The resonance numbering scheme corresponds to that in Fig. 3.

DISCUSSION

The previous neuronal cell culture studies on Zn_7-MT-3 and its mutant forms showed that both conserved Pro residues (Pro-7 and Pro-9) are necessary for the neuronal growth inhibitory activity exhibited by this MT isoform, as even single mutants were found to be inactive (30). The present mutational studies on Zn_7-MT-1 clearly established that besides the two prolines, the Thr-5 insert is also required for generating an MT-3-like inhibitory activity. The lack or substantial reduction of bioactivity exhibited by mutated MT-3 forms, in which Thr-5 was either removed or mutated to Ala (Fig. 1), corroborates the critical role of this residue. In general, because AD brain extract is added to neuronal cells in the bioassay, the possibility of threonine phosphorylation cannot be ruled out. However, because the T5A-MT-3 mutant still showed a low level of bioactivity, we currently favor a structural effect for this residue (see below). It should be noted, however, that the inhibitory activity of S6P,S8P+T5 MT-1 differs from that of MT-3 at high protein concentrations. Thus, whereas MT-3 negates the increased neuronal survival caused by AD brain extract (~50%) (13), the inhibitory activity of S6P,S8P+T5 MT-1 further increases (Fig. 1). However, because the mechanism of the biological assay for MT-3 is not understood, a quantitative comparison of the results is currently not possible. Nevertheless, the bioassay revealed that we have succeeded in engineering a gain-of-function in MT-1. Apart from the three critical residues introduced into MT-1, additional differences exist between the primary structures of MT-1 mutant and MT-3 (Table I). We suggest that both the resulting alterations of three-dimensional structures and of their reactivity may be important for this effect.

The similarity of the UV and MCD spectral features relative to wild-type and mutated MT-1 forms indicates that, in all cases, the nine cysteines of the β-domain are involved in the formation of a 3-metal cluster composed of tetrahedral Cd-$(Cys)_4$ centers. However, the changes observed in the CD spectra reflect an alteration of the wild-type MT-1 Cd_3S_9 cluster geometry upon the introduction of the two Pro residues into the sequence, with no additional changes occurring upon Thr-5 insertion. Deeper insights into the structure and dynamics of the 3-metal cluster in the modified N-terminal β-domain can be obtained from NMR studies. From the comparison of the ^{113}Cd NMR features of wild-type MT-1 and the mutant S6P,S8P MT-1, it can be concluded that the presence of the two critical proline residues affects the dynamics of the Cd_3S_9 cluster in the β-domain in a manner similar to that found in MT-3 (28). Thus,

the reduced signal intensities even at 323 K are in line with the generation of a fluctuating ensemble of cluster substrates, which remain non-detectable because of the slow exchange with the NMR-detectable cluster population and to excessive exchange broadening among the intrinsic conformational and configurational cluster substrates. We proposed previously (30) that the kinetic barrier for the exchange between the detectable and non-detectable ensemble of cluster substrates is due to the slow *cis*/*trans* interconversion of Cys-Pro amide bonds. By taking into consideration the conformational restraints imposed by the proline residues in a polypeptide chain (42), it is conceivable that the presence of the ^{6}CPCP^{9} motif in MT-3 and MT-1 mutants perturbs the geometrical requirements from the CysS-metal coordinative bonds within the Cd_3S_9 cluster, leading to a structure destabilization. Apart from the greater ease of prolyl *cis*/*trans*-isomerization, the structure destabilization would also account for the enhanced intersite metal exchange observed in the detectable cluster ensemble. This is in agreement with the recent multidimensional NMR studies (29) of MT-3, which show a restricted conformational flexibility in the 7 first residues of the β-domain together with high internal dynamics and conformational exchange within the rest of the domain.

The mutational insertion of Thr-5 into S6P,S8P MT-1 apparently does not further modify the cluster architecture (Fig. 2) and the solvent accessibility of the metal-ligated cysteines (see above). However, according to the NMR studies the dynamics of the N-terminal β-domain increases substantially. In particular, as judged by the reduced signal intensities at both temperatures (298 and 323 K), the non-detectable cluster population increases. This observation may be explained by the fact that the presence of Thr-5 enhances the kinetic barrier introduced by *cis*/*trans*-isomerization of Cys-Pro bond(s), owing either to the increase of the free energy of the transition state associated to this process or to the stabilization of the thereby generated NMR non-detectable cluster ensemble. The latter would be consistent with our preliminary molecular dynamics simulations on MT-1 mutants, which favor the formation of a side-chain-to-backbone hydrogen bond interaction involving Thr-5 only in a specific isomeric state of the prolyl residues.[2]

The present biological and structural studies reveal that the engineering of the MT-3 conserved motif, ^{5}TCPCP^{9}, into the inactive MT-1 isoform, brings about the neuronal activity and unprecedented cluster dynamics recognized in the β-domain of MT-3. The fact that, in spite of about 70% sequence identity between MT-1 and MT-3, the introduction of the three critical amino acid residues into MT-1 is both necessary and sufficient for the generation of neuronal growth inhibitory activity is striking. MTs belong to a growing class of proteins with a nonregular protein structure under physiological conditions (43). In this context, there is increasing awareness of compact but incompletely folded states of proteins that contain much of the native secondary structure but lack fixed tertiary interactions, playing an important role in many cellular processes (44). Based on our studies it would appear that MT-3 bioactivity resides in the kinetically trapped and intrinsically disordered cluster ensemble induced by the presence of the ^{5}TCPCP^{9} motif. The described dynamic model could be envisaged as being relevant to a biological process requiring recognition of a specific spatial arrangement. The proline-rich motif could provide the scaffolding or the platform for an interaction with another so far unknown component present in the brain extract (45). Taken together, the results provide a basis for understanding the widely different function of this isoform and clearly suggest that the structure/cluster dynamics is required for MT-3 bioactivity. These observations raise intriguing questions as to the role of metal cluster disorder in biological processes.

Acknowledgments—We thank N. Walch and S. Jurt for recording the NMR spectra.

[2] B. Oliva, N. Romero-Isart, and M. Vašák, manuscript in preparation.

REFERENCES

1. Selkoe, D. J. (2001) *Physiol. Rev.* **81,** 741–766
2. Ihara, Y. (1988) *Brain Res.* **459,** 138–144
3. De Strooper, B., Saftig, P., Craessaerts, K., Vanderstichele, H., Guhde, G., Annaert, W., Von Figura, K., and Van Leuven, F. (1998) *Nature* **391,** 387–390
4. Vallee, B. L. (1995) *Neurochem. Int.* **27,** 23–33
5. Vašák, M., and Hasler, D. W. (2000) *Curr. Opin. Chem. Biol.* **4,** 177–183
6. Hidalgo, J., Aschner, M., Zatta, P., and Vašák, M. (2001) *Brain Res. Bull.* **55,** 133–145
7. Uchida, Y., Takio, K., Titani, K., Ihara, Y., and Tomonaga, M. (1991) *Neuron* **7,** 337–347
8. Carrasco, J., Giralt, M., Molinero, A., Penkowa, M., Moos, T., and Hidalgo, J. (1999) *J. Neurotrauma* **16,** 1115–1129
9. Sewell, A. K., Jensen, L. T., Erickson, J. C., Palmiter, R. D., and Winge, D. R. (1995) *Biochemistry* **34,** 4740–4747
10. Uchida, Y., and Ihara, Y. (1995) *J. Biol. Chem.* **270,** 3365–3369
11. Bruinink, A., Faller, P., Sidler, C., Bogumil, R., and Vašák, M. (1998) *Chem. Biol. Interact.* **115,** 167–174
12. Tsuji, S., Kobayashi, H., Uchida, Y., Ihara, Y., and Miyatake, T. (1992) *EMBO J.* **11,** 4843–4850
13. Erickson, J. C., Sewell, A. K., Jensen, L. T., Winge, D. R., and Palmiter, R. D. (1994) *Brain Res.* **649,** 297–304
14. Hozumi, I., Inuzuka, T., Hiraiwa, M., Uchida, Y., Anezaki, T., Ishiguro, H., Kobayashi, H., Uda, Y., Miyatake, T., and Tsuji, S. (1995) *Brain Res.* **688,** 143–148
15. Kohmura, E., Yuguchi, T., Sakaki, T., Yamashita, T., Nonaka, M., and Hayakawa, T. (1997) *Restor. Neurol. Neurosci.* **11,** 169–175
16. Erickson, J. C., Hollopeter, G., Thomas, S. A., Froelick, G. J., and Palmiter, R. D. (1997) *J. Neurosci.* **17,** 1271–1281
17. Montoliu, C., Monfort, P., Carrasco, J., Palacios, O., Capdevila, M., Hidalgo, J., and Felipo, V. (2000) *J. Neurochem.* **75,** 266–273
18. Irie, Y., and Keung, W. M. (2001) *Biochem. Biophys. Res. Commun.* **282,** 416–420
19. Palmiter, R. D., Findley, S. D., Whitmore, T. E., and Durnam, D. M. (1992) *Proc. Natl. Acad. Sci. U. S. A.* **89,** 6333–6337
20. Zheng, H., Berman, N. E., and Klaassen, C. D. (1995) *Neurochem. Int.* **27,** 43–58
21. Masters, B. A., Quaife, C. J., Erickson, J. C., Kelly, E. J., Froelick, G. J., Zambrowicz, B. P., Brinster, R. L., and Palmiter, R. D. (1994) *J. Neurosci.* **14,** 5844–5857
22. Palmiter, R. D. (1995) *Toxicol. Appl. Pharmacol.* **135,** 139–146
23. Quaife, C. J., Kelly, E. J., Masters, B. A., Brinster, R. L., and Palmiter, R. D. (1998) *Toxicol. Appl. Pharmacol.* **148,** 148–157
24. Amoreux, M. C., Van Gool, D., Herrero, M. T., Dom, R., Colpaert, F. C., and Pauwels, P. J. (1997) *Mol. Chem. Neuropathol.* **32,** 101–121
25. Yu, W. H., Lukiw, W. J., Bergeron, C., Niznik, H. B., and Fraser, P. E. (2001) *Brain Res.* **894,** 37–45
26. Braun, W., Vašák, M., Robbins, A. H., Stout, C. D., Wagner, G., Kägi, J. H., and Wüthrich, K. (1992) *Proc. Natl. Acad. Sci. U. S. A.* **89,** 10124–10128
27. Zangger, K., Öz, G., Otvos, J. D., and Armitage, I. M. (1999) *Protein Sci.* **8,** 2630–2638
28. Faller, P., Hasler, D. W., Zerbe, O., Klauser, S., Winge, D. R., and Vašák, M. (1999) *Biochemistry* **38,** 10158–10167
29. Öz, G., Zangger, K., and Armitage, I. M. (2001) *Biochemistry* **40,** 11433–11441
30. Hasler, D. W., Jensen, L. T., Zerbe, O., Winge, D. R., and Vašák, M. (2000) *Biochemistry* **39,** 14567–14575
31. Vašák, M. (1991) *Methods Enzymol.* **205,** 452–458
32. Pedersen, A. O., and Jacobsen, J. (1980) *Eur. J. Biochem.* **106,** 291–295
33. Vašák, M., Kägi, J. H., and Hill, H. A. (1981) *Biochemistry* **20,** 2852–2856
34. Coleman, J. E. (1993) *Methods Enzymol.* **227,** 16–43
35. Messerle, B. A., Schaffer, A., Vašák, M., Kägi, J. H., and Wüthrich, K. (1992) *J. Mol. Biol.* **225,** 433–443
36. Willner, H., Vašák, M., and Kägi, J. H. (1987) *Biochemistry* **26,** 6287–6292
37. Carson, G. K., Dean, P. A., and Stillman, M. J. (1981) *Inorg. Chim. Acta* **56,** 59–71
38. Bogumil, R., Faller, P., Binz, P. A., Vašák, M., Charnock, J. M., and Garner, C. D. (1998) *Eur. J. Biochem.* **255,** 172–177
39. Li, T. Y., Minkel, D. T., Shaw, C. F., III, and Petering, D. H. (1981) *Biochem. J.* **193,** 441–446
40. Hagen, K. S., Stephan, D. W., and Holm, R. H. (1982) *Inorg. Chem.* **21,** 3928–3936
41. Otvos, J. D., Engeseth, H. R., Nettesheim, D. G., and Hilt, C. R. (1987) *Experientia* (*Basel*) **52,** (suppl.) 171–178
42. Williamson, M. P. (1994) *Biochem. J.* **297,** 249–260
43. Smyth, E., Syme, C. D., Blanch, E. W., Hecht, L., Vašák, M., and Barron, L. D. (2001) *Biopolymers* **58,** 138–151
44. Wright, P. E., and Dyson, H. J. (1999) *J. Mol. Biol.* **293,** 321–331
45. Kay, B. K., Williamson, M. P., and Sudol, M. (2000) *FASEB J.* **14,** 231–241